Cellular & Molecular Immunology (2017) 14, 685–692

www.nature.com/cmi

RESEARCH ARTICLE

Trap1a is an X-linked and cell-intrinsic regulator of thymocyte development

Chi-Shan Li[1,5], Fei Tang[2,5], Peng Zhang[3], Taijiao Jiang[3], Thomas L Saunders[4], Pan Zheng[2] and Yang Liu[2]

The X-linked *Trap1a* gene encodes the tumor rejection antigen P1A, which is expressed in fetal tissues and multiple lineages of tumor cells. The function of this gene remains unknown. Using chimeric mice with wild-type (WT) and *Trap1a*$^{-/y}$ bone marrow, we show that *Trap1a*$^{-/y}$ donor cells are capable of generating most lineages of hematopoietic cells, with the notable exception of T cells. Deletion of *Trap1a* selectively arrests T-cell development at double-negative stage 1 (DN1, with a CD4$^-$CD8$^-$CD25$^-$CD44$^+$ phenotype). Because *Trap1a* is expressed in Lin$^-$Sca-1$^+$c-Kit$^+$ and common lymphoid progenitors but not in immature thymocytes (DN1-DN4), *Trap1a* mutations affect the differentiation potential of progenitor cells without directly acting on T cells. Despite a similarity in the blockade of DN1 to DN2 transition, the *Trap1a*$^{-/y}$ DN1 cells have normal expression of c-Kit, in contrast to what was reported in the *Notch1*$^{-/-}$ DN1. Complementary DNA profiling of *Trap1a*$^{-/y}$ and WT embryonic stem cells shows that *Trap1a* does not regulate the Notch pathway. Our data reveal that *Trap1a* is an X-linked regulator that affects the differentiation potential of progenitor cells into T cells through a Notch-independent mechanism and identify an important function for the *Trap1a* gene.
Cellular & Molecular Immunology (2017) **14,** 685–692; doi:10.1038/cmi.2015.108; published online 11 April 2016

Keywords: Notch; tumor antigens; T cell development

INTRODUCTION

Thymopoiesis consists of both the orderly differentiation and rapid expansion of T-cell progenitors arriving from peripheral blood.[1] The early differentiation of immature thymocytes can be marked by the expression of CD44 and CD25 among the CD3$^-$CD4$^-$CD8$^-$ thymocytes.[2] Recent studies suggest that a subset of blood Lin$^-$Sca1$^+$c-Kit$^+$ cells (LSK) are likely the precursors of thymocytes. In the thymus, the LSK are part of the double-negative stage 1 (DN1) (CD44$^+$CD25$^-$) subset.[1] Notch/RBP-J signaling is responsible for commitment of progenitors to T-cell lineage (early T-cell progenitor) and the transitions of early T-cell progenitorsfrom DN1 to DN2 (CD44$^+$CD25$^+$) and from DN3 (CD44$^-$CD25$^+$) to DN4 (CD44$^-$CD25$^-$).[3] Notch/RBP-J signaling also controls the massive expansion of immature thymocytes.[4]

The X-linked *Trap1a* gene encodes the first known tumor antigen (P1A) recognized by cytotoxic T cells in mice[5] and is overexpressed in multiple lineages of tumor cells.[6] P1A is known to be overexpressed in the testis, placenta[7,8] and embryonic stem (ES) cells (this study). We reported that the transgenic overexpression of *Trap1a* is sufficient to cause thymic lymphoma in an immune-deficient host.[9] However, the physiological function of P1A remains largely unknown due to the lack of genetic models. To address this issue, we produced ES cells with a floxed *Trap1a* locus. Because these ES cells were not germline-transmitted, we analyzed the contribution of these mutant ES cells to various tissues in chimeras. Using both blastocyst and bone marrow (BM) chimeras, we observed an unexpected cell-autonomous function of P1A in early thymocyte differentiation, specifically in the DN1 to DN2 transition. Our data reveal an X-linked regulator of the DN1 to DN2 transition in thymocyte development.

MATERIALS AND METHODS

Generation of *Trap1a*$^{-/y}$ mutant ES cells

A mouse *Trap1a* genomic clone was obtained by screening a 129/SvJ BAC library. A neomycin/TK cassette flanked by two

[1]Institute of Biomedical Sciences, Academia Sinica, Taipei, Taiwan, China; [2]Center for Cancer and Immunology Research, Children's National Medical Center, Washington, DC, USA; [3]Institute of Biophysics, Chinese Academy of Science, Beijing, China and [4]Department of Internal Medicine, School of Medicine, University of Michigan, Ann Arbor, MI, USA
[5]These authors contributed equally to this work.
Correspondence: Professor P Zheng or Professor Y Liu, Center for Cancer and Immunology Research, Children's National Medical Center, Washington, DC, USA.
E-mail: pzheng@cnmc.org or yaliu@cnmc.org
Received: 12 October 2015; Revised: 25 November 2015; Accepted: 25 November 2015

LoxP sites was cloned between Exon 1 and Exon 2, introducing a new *Bam*HI site for genotyping purposes. A third LoxP site was located before Exon 1. This construct was electroporated into murine male X:Y R1 ES cells,[10] and homologous recombination was confirmed by Southern blot analysis after *Bam*HI digestion. Positive ES cell clones were then electroporated with a Cre vector to eliminate the neomycin/TK cassette and *Trap1a* Exon 1 (Figure 1a). ES cells were co-cultured with mouse embryonic fibroblast feeder cells in Dulbecco's modified Eagle's medium containing 15% fetal calf serum, 0.1 mM β-mercaptoethanol, 10^3 u/ml leukemia inhibitory factor and 4 mM glutamine as previously described.[11]

Contribution of mutant ES cells to different organs

Trap1a$^{-/y}$ ES cells (CD45.2) were microinjected into B6.SJL-PtprcaPep3b/BoyJ blastocysts (CD45.1) by the Transgenic Animal Model Core at the University of Michigan. The resulting pups were assessed initially for chimerism based on coat coloration. Genomic DNA was isolated from tissues of chimeric mice using a DNeasy Blood & Tissue Kit (Qiagen, Valencia, CA, USA). ES cell contribution was initially tested by quantitative PCR. The contribution of *Trap1a*$^{-/y}$ ES cells to various tissues of chimeric mice was determined by using primers specific for the LoxP site. The amount of *Trap1a* Exon 2 was used as an internal control. The contribution ratio of *Trap1a*$^{-/y}$ ES cells in different organs was calculated as 2 to the power of the Ct value of the specific LoxP site subtracted from the corresponding Ct value of the P1A Exon 2. This value was normalized against the value from *Trap1a*$^{-/y}$ ES cells, which is defined as 100%. The following primers were used for detecting the LoxP site: forward, 5′-CCCTAATGTATGCTATA CGAAGTTAT-3′; reverse, 5′-GGGGTCCTGTAAAGGAAAGG-3′ The following primers were used for *Trap1a* Exon 2: forward, 5′-TCCACGACCCTAATTTCC-3′; reverse, 5′-GCATGCCTAA GGTGAGAAGC-3′.

Reverse transcription (RT)-PCR

Total RNA was isolated from *Trap1a*$^{+/y}$ and *Trap1a*$^{-/y}$ ES cells using a RNeasy Mini Kit (Qiagen). Complementary DNA was

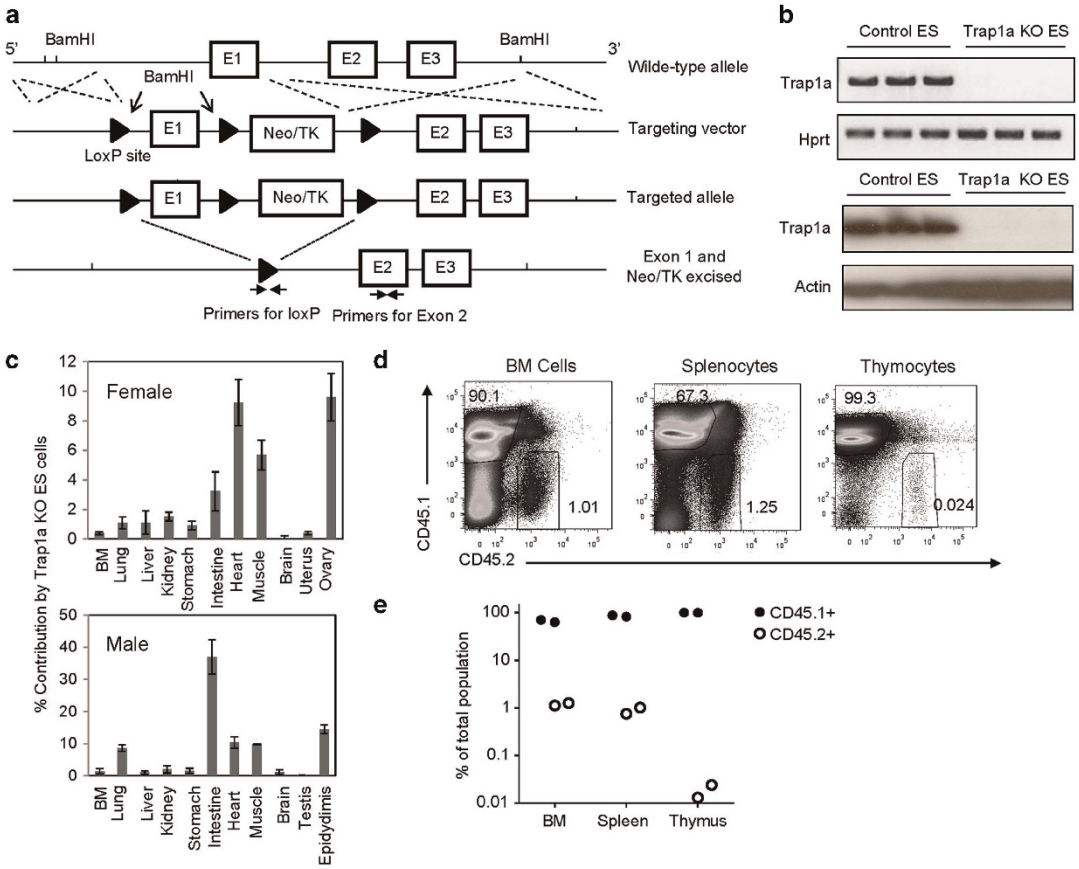

Figure 1 Contribution of *Trap1a*$^{-/y}$ ES cells to mouse tissues through blastocyst chimera analysis. (**a**) Diagram of constructs and mutant alleles. (**b**) Confirmation of *Trap1a* inactivation in ES cell clones by RT-PCR and western blot analysis. The *Trap1a*$^{fl/y}$ ES cells were electroporated with a vector expressing *Cre* recombinase. Three clones in control and Cre-transduced groups were compared for RNA and protein expression. (**c**) Contribution of *Trap1a*$^{-/y}$ ES cells to various tissues and organs. Chimera mice with greater than 50% contribution based on coat color were analyzed for contribution of *Trap1a*$^{-/y}$ cells based on quantitative PCR. (**d**) Flow cytometric quantitation of *Trap1a*$^{-/y}$ (CD45.2$^+$) hematopoietic cells in the BM, spleen and thymus. Data from the female chimera mouse are presented; similar results were obtained in the male chimera. (**e**) % Contribution of CD45.2$^+$ cells in the male and female chimera mice. BM, bone marrow; ES cells, embryonic stem cells; RT-PCR, reverse transcriptase-polymerase chain reaction.

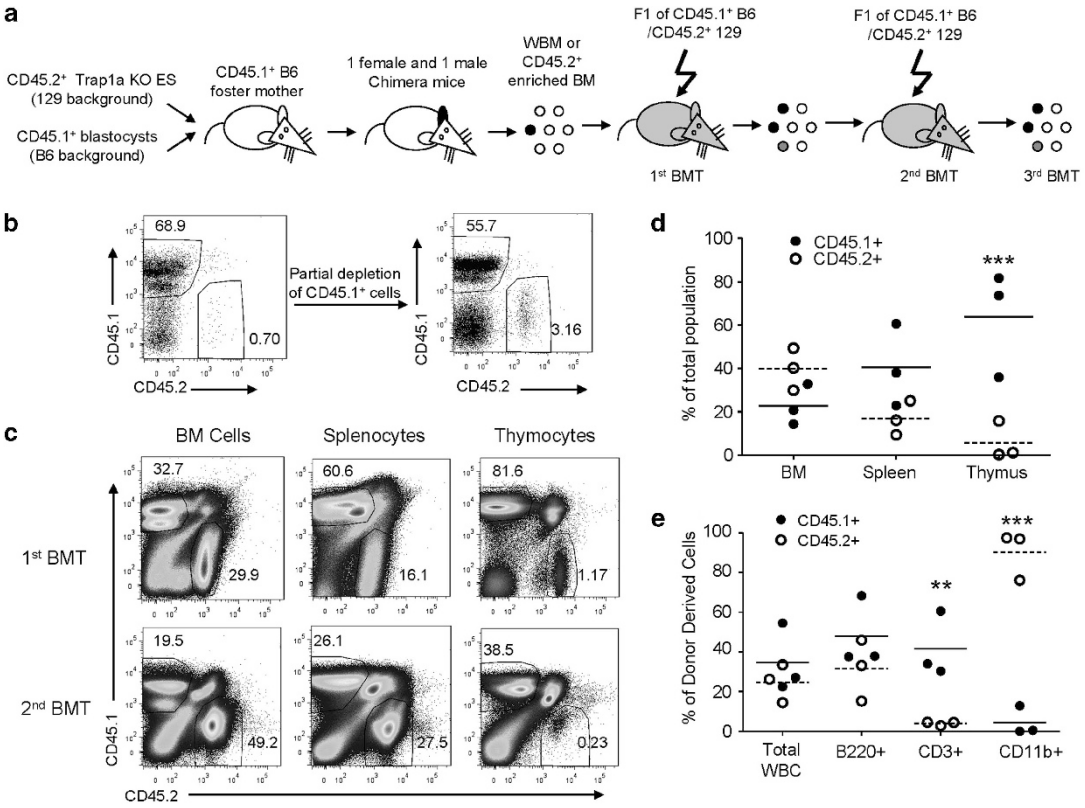

Figure 2 Cell-autonomous and long-lasting effect of *Trap1a* mutation on thymocyte production. (**a**) Diagram of experimental design. (**b**) Evidence of partial enrichment of mutant bone marrow cells by negative selection with anti-CD45.1 beads. (**c**) Impact of *Trap1a* mutation on thymocyte production in serial transplantation. Data shown are representative profiles of first and second transplantation. (**d**) Selective reduction of thymocyte production after *Trap1a* deletion. Data shown are % of WT and *Trap1a*$^{-/y}$ leukocytes at 4 or 11 weeks after second transplantation. (**e**) *Trap1a* deletion causes selective reduction of T cells and increase of myeloid cells in the peripheral blood at 11 weeks after second transplantation. $^{**}P<0.01$; $^{***}P<0.001$. WT, wild type.

synthesized using a SuperScript first-strand synthesis system kit (Invitrogen). For quantitative PCR, the expression of *Trap1a* was amplified by the forward primer 5′-AGAGATGAGCGTGG AAATGG-3′ and the reverse primer 5′-CAGGAAATTAGGGT CGTGGA-3′. The *Hprt* gene was used as an internal control, and the primers were 5′-CAGGCCAGACTTTGTTGGAT-3′ (forward) and 5′-GCGCTCATCTTAGGCTTTGT-3′ (reverse). For conventional PCR, primers specific for *Trap1a* (forward: 5′-ATCTAGGGTGGCTGGTCTTC-3′; reverse: 5′-CCATTTCC TCTTCCTCCTCC-3′) were used to validate its expression in the mouse LSK population.

Western blot analysis

Samples were lysed in protein lysis buffer (50 mM Tris-HCl, pH 7.4, 150 mM NaCl, 0.5% NP-40), and protease inhibitor cocktails (Sigma, St Louis, MO, USA) including 4-(2-aminoethyl) benzenesulfonyl fluoride hydrochloride, Aprotinin, Bestatin, E-64, Leupeptin and Pepstatin A were added. Cell lysates were prepared and 50 μg of protein per lane was loaded and separated by 10% sodium dodecyl sulfate-polyacrylamide gel electrophoresis, transferred to polyvinylidene fluoride membranes, and incubated with corresponding antibodies, including rabbit anti-P1A antibody[9] (1:500 dilution), anti-actin mouse antibody (Sigma, clone AC-15, 1:5000 dilution). Anti-rabbit or anti-mouse IgG horseradish peroxidase-linked antibody at 1:3500 dilution (GE Healthcare, Little Chalfont, UK) was used as a secondary antibody. Antibodies were detected with a chemiluminescence reaction using an enhanced chemiluminescence kit (Amersham Biosciences, Little Chalfont, UK) and visualized with exposure to film.

BM transplantation

Because *Trap1a*$^{-/y}$ ES only contributed ~1% to bone marrow cells in the chimeric mice, some experiments used anti-fluorescein isothiocyanate microbeads (Miltenyi Biotec, San Diego, CA, USA) to partially delete fluorescein isothiocyanate-labeled CD45.1^{+} cells and enrich the CD45.2^{+}*Trap1a*$^{-y}$ cell population. After CD45.2 enrichment, or without enrichment, a total of 5-7 × 10^{6} chimeric BM cells were injected intravenously into lethally irradiated (129/Sv × C57BL/6) F1 mice (CD45.1^{+} CD45.2^{+}) by a ^{137}Cs γ-ray source delivering a total of 1100 rads. All animal experiments were conducted in accordance with accepted standards of animal care and approved by the Institutional Animal Care and Use Committee of the University of Michigan and the Children's National Medical Center Research Institute.

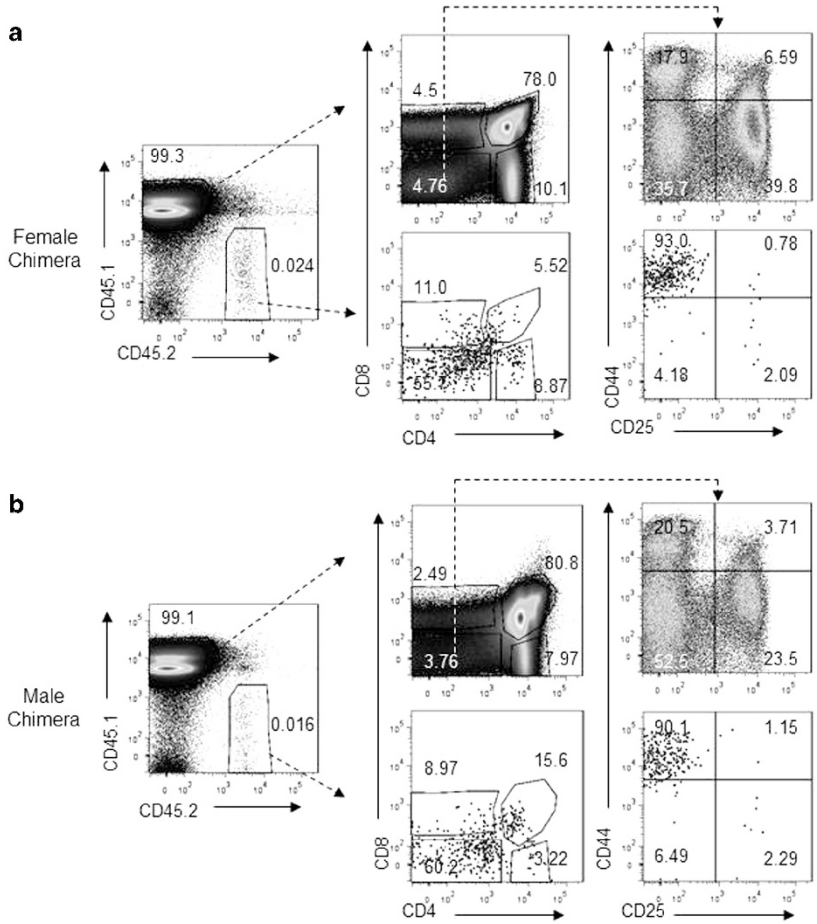

Figure 3 Selective blockade of DN1-DN2 transition by *Trap1a* deletion as revealed by flow cytometry. Data shown are profiles of thymocytes from the female (**a**) and male (**b**) blastocyst chimera mice.

Flow cytometric analysis and cell sorting

Peripheral blood was collected from the orbital sinus of mice. BM cells were collected from the tibia and femur of hind legs. Spleen and thymus were homogenized and passed through a cell strainer to generate a single-cell suspension. Cells were stained in phosphate-buffered saline plus 2% fetal bovine serum for 20 min on ice with fluorochrome-conjugated monoclonal antibodies (mAbs) at 1:200 or 1:100 dilution. The following mAbs from BD Biosciences (San Diego, CA, USA), eBioscience (San Diego, CA, USA) or BioLegend (San Diego, CA, USA) were used: anti-CD45.1 (A20), anti-CD45.2 (104), anti-CD3 (145-2C11), anti-CD4 (GK1.5), anti-CD8 (53-6.7), anti-CD25 (PC61.5), anti-CD44 (IM7), anti-CD11b (M1/70), anti-B220 (RA3-6B2), anti-TER-119 (TER-119), anti-Gr-1 (RB6-8C5), anti-Sca-1 (D7) and anti-c-Kit (2B8). After surface staining, cells were subsequently analyzed with a BD LSR II flow cytometer. The data were analyzed using FlowJo software (Tree Star, San Diego, CA, USA). Cell sorting was performed using a FACSAria (BD Biosciences).

cDNA microarray analysis

Gene expression profiling analysis of *Trap1a*$^{+/y}$ and the *Trap1a*$^{-/y}$ ES cells was carried out using an Affymetrix GeneChip Mouse Genome 430 2.0 array. The RNA samples were sent to the Affymetrix (Cleveland, OH, USA) and Microarray Core Facility at the University of Michigan for full service sample preparation. Probe intensities were measured and then processed with Affymetrix GeneChip operating software into image analysis (CEL) files. The Affymetrix CEL files were normalized using the Robust Multi-array Averaging method[12] and affy.[13] Then, we used limma[14] to identify differentially expressed genes. Functional analysis (gene ontology enrichment) of differentially expressed genes was assessed using the DAVID database (http://david.abcc.ncifcrf.gov/).

In silico data analysis

The RNA-seq raw data of thymocytes (double negative (DN) cells, double positive cells and natural regulatory T cells) were accessed through GEO Series accession number GSE48138.[15] Alignment of sequencing reads to the reference genome (version mm10) was performed using TopHat.[16] Then, the gene expression level was measured by RPKM and calculated by DEGseq.[17] The expression values of hematopoietic stem cells, LSK and common lymphoid progenitors (CLP) were extracted from the expression result file through GEO Series accession numbers GSE50896[18] and GSE50739.[19]

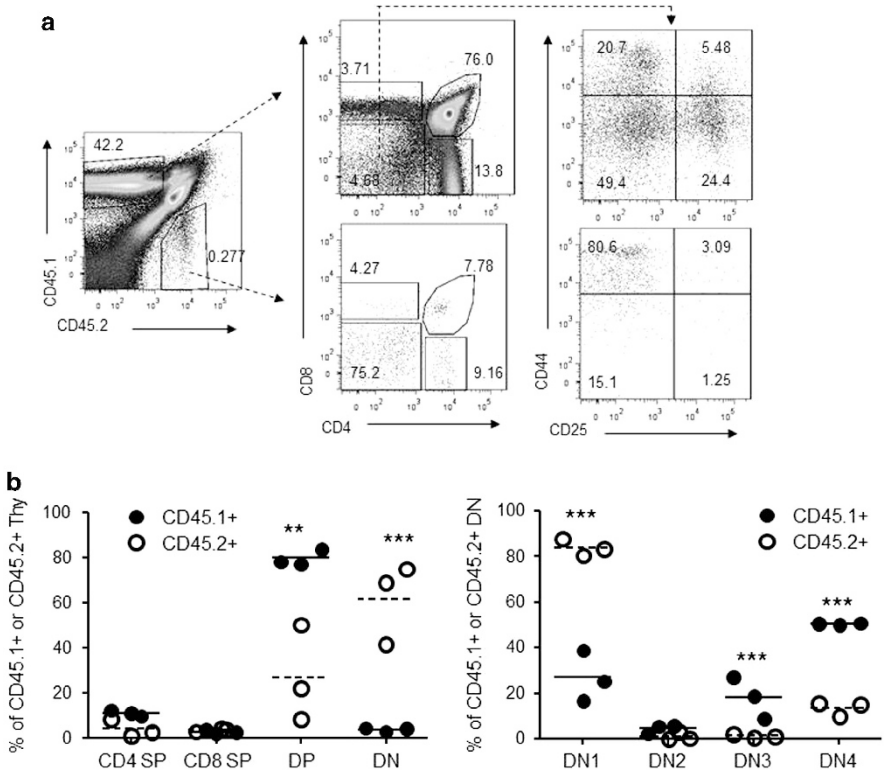

Figure 4 Cell-intrinsic *Trap1a* mutation is responsible for blockade of DN1-DN2 transition. (**a**) Representative profile of bone marrow chimera mouse at 11 weeks after the second round of transplantation. (**b**) Accumulation of DN1 cells in *Trap1a*$^{-/y}$ thymocytes. The thymocytes were harvested respectively at 11 or 12 weeks after the second round of transplantation or 7 months after the first round of transplantation.

Statistics

Data (shown as bar graphs) are presented as the mean ± s.e.m. (Figure 1c) or mean ± s.d. (Figure 5e). Two-tailed Student *t*-tests were used for comparison between the two experimental groups. Solid lines and dotted lines in the scatter plots represent mean values for the indicated groups. Statistical significance was determined as $^{*}P<0.05$, $^{**}P<0.01$ and $^{***}P<0.001$.

RESULTS

Chimera analysis revealed differential contributions of *Trap1a*-deficient ES cells to different organs

To understand the function of *Trap1a*, we generated ES cell lines containing a *Trap1a* triple LoxP gene-targeting vector that included a selectable neomycin/TK cassette and LoxP-flanked *Trap1a* Exon 1 in the mouse X chromosome (Figure 1a). ES clones devoid of P1A protein were obtained by electroporation with a Cre recombinase expression vector (Figure 1b). Unfortunately, the ES cells did not give germline transmission even before *Trap1a* deletion despite repeated attempts, perhaps because the neomycin/TK cassette may have subtly affected *Trap1a* expression in the hemizygous male-derived ES cells.

As an alternative approach, we removed the neomycin/TK cassette and the *Trap1a* Exon 1 by electroporation with a Cre recombinase expression vector into ES cells. Cre excised the intervening DNA segment and resulted in a single remaining LoxP site (Figure 1a). Several single *Trap1a*-null clones were selected and cultured for further analysis. As shown in Figure 1b by RT-PCR and western blotting, we successfully knocked out *Trap1a* expression in ES cells after removing *Trap1a* Exon 1. This deletion did not affect ES cell colony morphology or growth rate (Supplementary Figure S1). Moreover, the mutant ES cells formed teratomas of comparable sizes to those derived from WT ES cells. Moreover, histological analyses demonstrated that the mutant ES cells were capable of forming mesoderm, endoderm, ectoderm and germ cells (Supplementary Figure S2).

To determine whether *Trap1a*$^{-/y}$ ES cells could contribute to different organs, we injected them (derived from 129 ES cell line R1, CD45.2) into C57BL/6 (CD45.1) WT blastocysts. We characterized two chimeras with greater than 50% coat color contribution from *Trap1a*$^{-/y}$ ES cells. Through qPCR, the contribution ratio of *Trap1a*$^{-/y}$ ES cells in different organs was calculated as 2 to the power of the Ct value of the specific LoxP site subtracted from the corresponding Ct value of P1A Exon 2 (internal control). This value was normalized against the value from *Trap1a*$^{-/y}$ ES cells, which is defined as 100%. The organs and tissues that we analyzed included the lung, liver, kidney, stomach, intestine, heart, muscle, brain, uterus, ovary, testis, epididymis and BM. The primer positions are depicted in the upper panel of Figure 1c. As shown in the lower panel of Figure 1c, the *Trap1a*$^{-/y}$ ES cells contributed to various internal organs, although the contribution ratios differed among organs. Consistent with its abundant expression in the

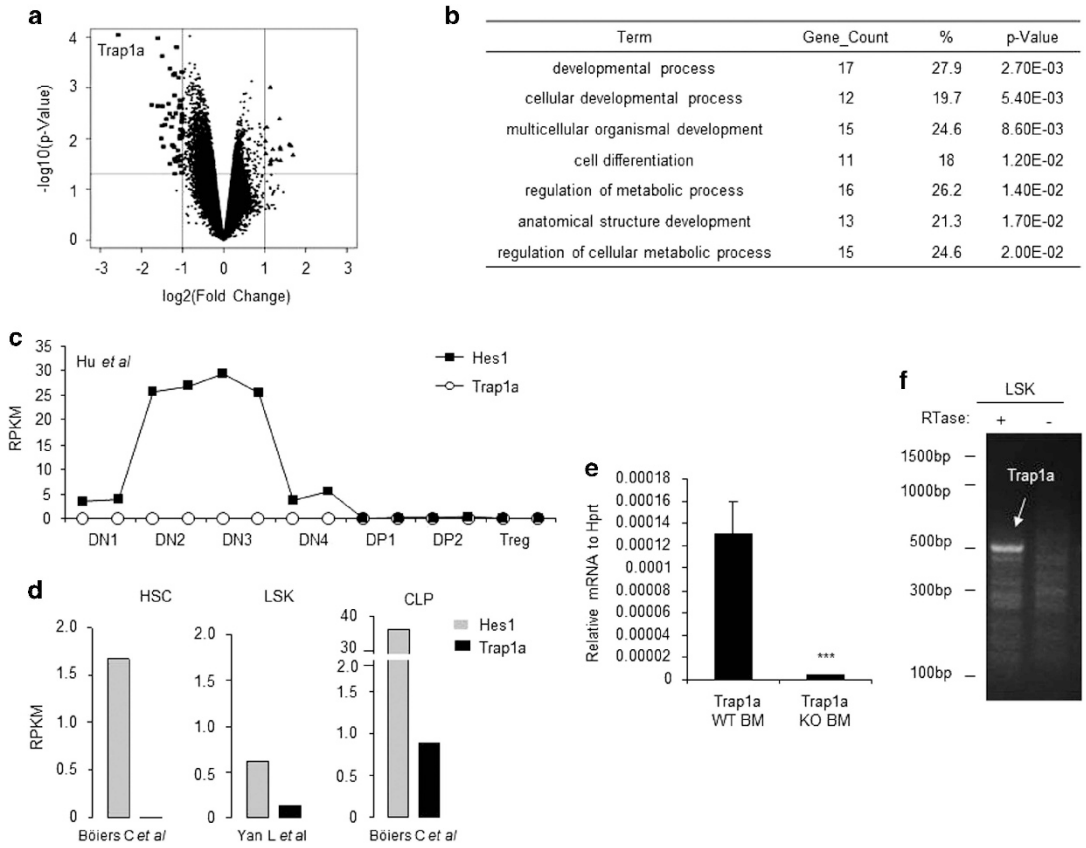

Term	Gene_Count	%	p-Value
developmental process	17	27.9	2.70E-03
cellular developmental process	12	19.7	5.40E-03
multicellular organismal development	15	24.6	8.60E-03
cell differentiation	11	18	1.20E-02
regulation of metabolic process	16	26.2	1.40E-02
anatomical structure development	13	21.3	1.70E-02
regulation of cellular metabolic process	15	24.6	2.00E-02

Figure 5 Function of *Trap1a* gene based on global expression analysis. (**a**) Identification of genes that are affected by *Trap1a* deletion in ES cells. The X-axis shows the ratios of expression levels between WT and *Trap1a*$^{-/y}$ ES cells, while the Y-axis shows –log10 *P* values. The large symbols indicate genes that are either upregulated (triangles) or downregulated (squares) by *Trap1a* deletion. (**b**) Functional enrichment analysis suggests that *Trap1a* may be involved in cellular development and metabolic pathways. (**c**–**e**) *Trap1a* is expressed in LSK and CLP but not in thymocytes and hematopoietic stem cells. (**c**, **d**) *In silico* analyses of RNAseq data from previous publications. (**e**) qPCR analysis of bone, marrow cells sorted from bone marrow chimera mice. (**f**) RT-PCR verification of *Trap1a* expression in the sorted LSK from CD45.1 (WT) and CD45.2 (mutant) LSK. CLP, common lymphoid progenitor; LSK, Lin$^-$/SCA$^+$/Kit$^+$; qPCR, quantitative polymerase chain reaction; RT-PCR, reverse transcriptase-polymerase chain reaction.

testis,[20] *Trap1a*-deficient ES cells failed to contribute to testis tissues.

Using the CD45 congenic markers, we quantified the relative number of *Trap1a*$^{-/y}$ ES cell-derived cells in major hematopoietic tissues, including the BM, spleen and thymus. As shown in Figures 1d and e, the number of CD45.2 cells in the spleen and BM was ~1%. Surprisingly, the contribution to thymocytes was further reduced by 40-fold, to 0.024%. These data suggest that *Trap1a* may affect thymocyte development.

Cell-intrinsic function of *Trap1a* in thymocyte development

To determine whether the *Trap1a* gene function in hematopoiesis is cell-intrinsic, we transplanted BM cells from mouse chimeras (either CD45.1$^+$ or CD45.2$^+$) into lethally irradiated (129/Sv × C57BL/6) F1 mice (CD45.1$^+$CD45.2$^+$) (Figure 2a). In this setting, the WT cells were CD45.1$^+$CD45.2$^-$, the *Trap1a*$^{-/y}$ cells were CD45.1$^-$CD45.2$^+$, whereas the residual recipient leukocytes were CD45.1$^+$CD45.2$^+$ (Figure 2a). Because the number of CD45.2$^+$ BM cells in the female chimera was exceedingly low, we partially enriched CD45.1$^-$CD45.2$^+$cells by using negative selection (Figure 2b). This partial enrichment is sufficient because the proportion of stem/progenitor cells is higher among the mutant hematopoietic cells (data not shown). For comparison, male BM cells were directly used without enrichment. A similar trend was found with or without enrichment. We present data mainly from the female chimera because the higher proportion of mutant-derived cells in the female made the quantitation more reliable. As shown in Figure 2c, with the partial enrichment of CD45.1$^-$ CD45.2$^+$ donor cells, the proportions of mutant CD45.1$^-$ CD45.2$^+$ cells were comparable to WT CD45.1$^+$CD45.2$^-$ donor cells in the BM and spleen. However, the thymus was largely depleted of CD45.1$^-$CD45.2$^+$ cells (Figure 2c). The defects were even more striking in repeated transplantation (Figures 2c and d). The marked and selective reduction of thymocytes from the CD45.1$^-$CD45.2$^+$ donor, as summarized in Figure 2d, demonstrated a critical cell-intrinsic function of *Trap1a* in T-cell development. Consistent with a defective T-cell development, the proportion of T cells in the peripheral blood was also reduced, whereas that of myeloid cells was increased (Figure 2e).

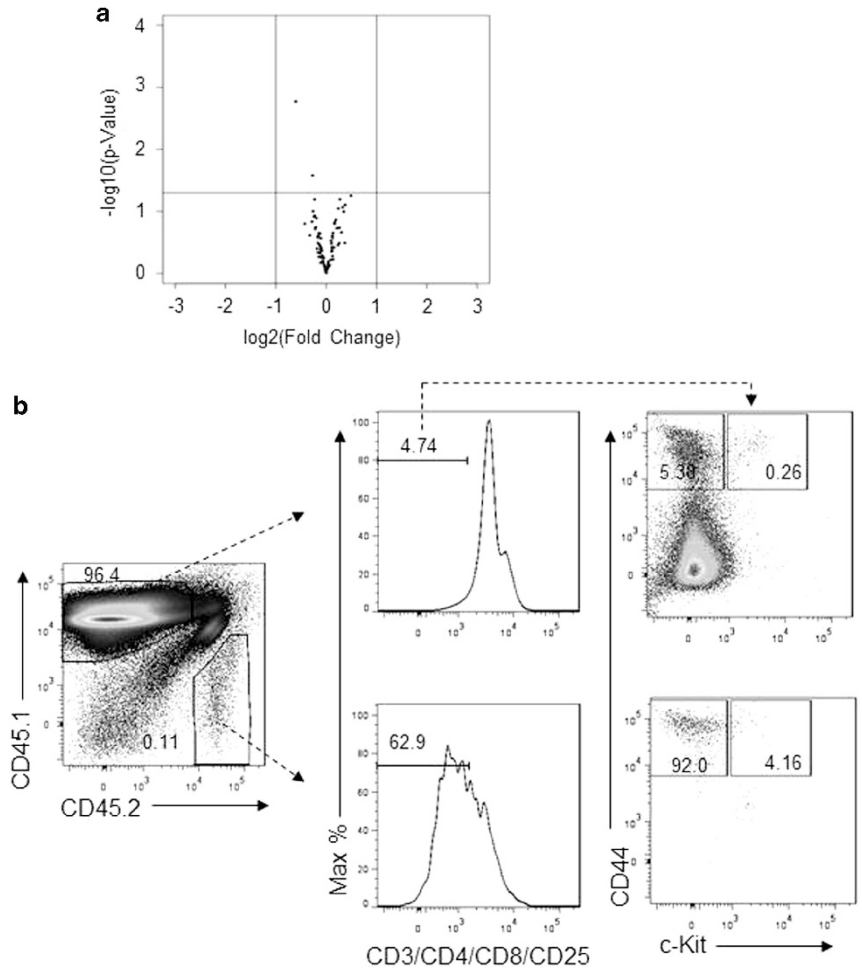

Figure 6 *Trap1a* mutation does not affect Notch signaling. (**a**) None of the 43 Notch signaling genes are affected by more than twofold. The X-axis shows the ratios of expression levels between WT and *Trap1a*$^{-/y}$ ES cells, while the Y-axis shows –log10 *P* values. (**b**) Distribution of c-Kit expression among the DN1 thymocytes from WT and *Trap1a*$^{-/y}$ stem cells. Data shown are representative profiles of thymocytes based on CD3/CD4/CD8/CD25/CD44 and c-Kit markers and have been reproduced in three independent experiments. ES cells, embryonic stem cells; WT, wild type.

A critical role for *Trap1a* in DN1 to DN2 transition

To understand which developmental stage is regulated by *Trap1a,* we further analyzed the thymocyte composition of the blastocyst mouse chimeras based on the expression of CD4, CD8, CD44 and CD25. As shown in Figure 3, although the CD4$^-$CD8$^-$ thymocytes were a minority among the WT cells (CD45.1$^+$), they represented the overwhelming majority of the CD45.2 thymocytes. After the CD4$^-$CD8$^-$ thymocytes were further subdivided into DN1-DN4 based on the distribution of CD44 and CD25 markers, it was clear that essentially all DN had a phenotype of CD44^{hi} CD25$^-$ in the CD45.2 thymocytes. The selective defects in the blastocyst chimera were substantiated in multiple rounds of BM transplantation (Figures 4a and b). Therefore, *Trap1a* deletion caused cell-intrinsic defects in DN1-DN2 transition.

Because there were too few *Trap1a*$^{-/y}$ thymocytes for expression profiling, we profiled the *Trap1a*$^{+/y}$ and the *Trap1a*$^{-/y}$ ES cells and compared the Notch signaling signature. Using twofold changes and a *P* value of 0.05 as the cutoff, we observed 51 downregulated genes and 17 upregulated genes after *Trap1a* deletion (Figure 5a and Supplementary Dataset 1). As expected, the most downregulated gene was *Trap1a*. Functional enrichment analysis suggested that these genes affect cellular metabolism and development (Figure 5b).

Theoretically, *Trap1a* may act directly either to promote the DN1-DN2 transition or to determine the potential of T-cell progenitors. The former predicts the expression of *Trap1a* in the thymocytes, whereas the latter does not have such a requirement. We carried out *in silico* analyses for *Trap1a* expression. As shown in Figure 5c, RNAseq data[15] showed that *Trap1a* was not expressed in thymocytes, whereas databases generated by others[18,19] revealed low levels of expression in BM LSK stem/progenitor cells and CLP cells (Figure 5d). Because thymocyte progenitors were identified as part of the LSK population,[21] we used PCR to validate *Trap1a* expression in LSK cells. As shown in Figure 5e, *Trap1a* was detected in the WT but not the CD45.2$^+$ mutant BM cells by qPCR. Further investigation by conventional PCR confirmed the expression of

Trap1a in sorted LSK cells from the BM of WT mice (Figure 5f). Therefore, the expression pattern suggested that *Trap1a* affects the potential of T cell progenitors rather than directly acting on DN1 to promote the DN1 to DN2 transition.

The nearly complete inhibition of the DN1 to DN2 transition is reminiscent of the phenotype of *Notch1*$^{-/-}$ thymocytes.[4] To determine whether the Notch signaling pathway was affected, we compared the expression of genes involved in Notch pathways in *Trap1a*$^{+/y}$ and *Trap1a*$^{-/y}$ ES cells. As shown in Figure 6a and Supplementary Dataset 2, none of the genes in the Notch pathway were affected by twofold or more. Because *Notch1* deletion eliminated c-Kit expression in DN1 cells,[21] we compared the expression of c-Kit in DN1 thymocytes. As shown in Figure 6b, the distribution of c-Kit expression in DN1 was unaffected by *Trap1a* deletion. These data suggest that *Trap1a* deletion does not affect thymocyte development through inhibition of Notch signaling.

DISCUSSION

Taken together, our data revealed *Trap1a* as a new regulator of the DN1-DN2 transition. This checkpoint is distinct from *Notch1* signaling at three levels. First, phenotypically, *Notch1*-deficient DN1 thymocytes were blocked prior to the expression of c-Kit, the earliest marker of T-cell progenitors, whereas the *Trap1a*-deficient thymocytes had normal expression of c-Kit. Second, although Notch signaling is active at the DN1-DN4 based on the expression of its target genes, *Trap1a* is expressed only in progenitor cells before they reach the thymus. Third, gene signature analysis of ES cells suggests that *Trap1a* deletion does not affect the expression of genes involved in Notch signaling. It is intriguing to note that because *Trap1a* expression cannot be found in developing thymocytes the potential for T-cell fate can be determined before T-cell progenitors reach the thymus.

P1A was the first tumor antigen to be identified. However, no physiological function has been attributed to P1A. By showing a critical role for P1A in T-cell development, our study filled in this major gap. Furthermore, based on the lack of contribution of the *Trap1a*$^{-/y}$ ES cells to several tissues, particularly the uterus, testis and brain, it is likely that P1A plays a fundamental role in the development of vital organs. Additional studies will be needed to determine the molecular mechanism by which P1A controls development of multiple cell types.

CONFLICT OF INTEREST

The authors declare no conflict of interest.

ACKNOWLEDGEMENTS

This work is supported by grants from the National Institutes of Health (AI64350, CA171972, CA58033 and AG036690).

1 Schwarz BA, Bhandoola A. Circulating hematopoietic progenitors with T lineage potential. *Nat Immunol* 2004; **5**: 953–960.
2 Ceredig R, Rolink T. A positive look at double-negative thymocytes. *Nat Rev Immunol* 2002; **2**: 888–897.
3 Schmitt TM, Ciofani M, Petrie HT, Zuniga-Pflucker JC. Maintenance of T cell specification and differentiation requires recurrent notch receptor-ligand interactions. *J Exp Med* 2004; **200**: 469–479.
4 Allman D, Karnell FG, Punt JA, Bakkour S, Xu L, Myung P *et al.* Separation of Notch1 promoted lineage commitment and expansion/transformation in developing T cells. *J Exp Med* 2001; **194**: 99–106.
5 Van den Eynde B, Lethe B, Van Pel A, De Plaen E, Boon T. The gene coding for a major tumor rejection antigen of tumor P815 is identical to the normal gene of syngeneic DBA/2 mice. *J Exp Med* 1991; **173**: 1373–1384.
6 Ramarathinam L, Sarma S, Maric M, Zhao M, Yang G, Chen L *et al.* Multiple lineages of tumors express a common tumor antigen, P1A, but they are not cross-protected. *J Immunol* 1995; **155**: 5323–5329.
7 Boon T, Cerottini JC, Van den Eynde B, van der Bruggen P, Van Pel A. Tumor antigens recognized by T lymphocytes. *Annu Rev Immunol* 1994; **12**: 337–365.
8 Brandle D, Bilsborough J, Rulicke T, Uyttenhove C, Boon T, Van den Eynde BJ. The shared tumor-specific antigen encoded by mouse gene P1A is a target not only for cytolytic T lymphocytes but also for tumor rejection. *Eur J Immunol* 1998; **28**: 4010–4019.
9 Li CS, Chen C, Zheng P, Liu Y. Transgenic expression of P1A induced thymic tumor: a role for onco-fetal antigens in tumorigenesis. *PLoS One* 2010; **5**: e13439.
10 Nagy A, Rossant J, Nagy R, Abramow-Newerly W, Roder JC. Derivation of completely cell culture-derived mice from early-passage embryonic stem cells. *Proc Natl Acad Sci USA* 1993; **90**: 8424–8428.
11 Hughes ED, Saunders TL. *Gene Targeting in Embryonic Stem Cells*. Springer-Verlag: Berlin. 2001.
12 Irizarry RA, Hobbs B, Collin F, Beazer-Barclay YD, Antonellis KJ, Scherf U *et al.* Exploration, normalization, and summaries of high density oligonucleotide array probe level data. *Biostatistics* 2003; **4**: 249–264.
13 Gautier L, Cope L, Bolstad BM, Irizarry RA. affy–analysis of Affymetrix GeneChip data at the probe level. *Bioinformatics* 2004; **20**: 307–315.
14 Ritchie ME, Phipson B, Wu D, Hu Y, Law CW, Shi W *et al.* limma powers differential expression analyses for RNA-sequencing and microarray studies. *Nucleic Acids Res* 2015; **43**: e47.
15 Hu G, Tang Q, Sharma S, Yu F, Escobar TM, Muljo SA *et al.* Expression and regulation of intergenic long noncoding RNAs during T cell development and differentiation. *Nat Immunol* 2013; **14**: 1190–1198.
16 Kim D, Pertea G, Trapnell C, Pimentel H, Kelley R, Salzberg SL. TopHat2: accurate alignment of transcriptomes in the presence of insertions, deletions and gene fusions. *Genome Biol* 2013; **14**: R36.
17 Wang L, Feng Z, Wang X, Zhang X. DEGseq: an R package for identifying differentially expressed genes from RNA-seq data. *Bioinformatics* 2010; **26**: 136–138.
18 Boiers C, Carrelha J, Lutteropp M, Luc S, Green JC, Azzoni E *et al.* Lymphomyeloid contribution of an immune-restricted progenitor emerging prior to definitive hematopoietic stem cells. *Cell Stem Cell* 2013; **13**: 535–548.
19 Yan L, Womack B, Wotton D, Guo Y, Shyr Y, Dave U *et al.* Tgif1 regulates quiescence and self-renewal of hematopoietic stem cells. *Mol Cell Biol* 2013; **33**: 4824–4833.
20 Uyttenhove C, Godfraind C, Lethe B, Amar-Costesec A, Renauld JC, Gajewski TF *et al.* The expression of mouse gene P1A in testis does not prevent safe induction of cytolytic T cells against a P1A-encoded tumor antigen. *Int J Cancer* 1997; **70**: 349–356.
21 Tan JB, Visan I, Yuan JS, Guidos CJ. Requirement for Notch1 signals at sequential early stages of intrathymic T cell development. *Nat Immunol* 2005; **6**: 671–679.

Supplementary Information for this article can be found on the *Cellular & Molecular Immunology* website (http://www.nature.com/cmi)